Reduction of Frequency Fluctuation of Wind Farm Connected Power System by Adaptive Neural Network Controlled ECS

[1]S.M. Muyeen, [2]Hany M. Hasanien, and [1]J. Tamura

[1]*Department of EEE, Kitami Institute of Technology, 165 Koen Cho, Kitami, 090-8507, Hokkaido, Japan*

[2]*Dept. of Elec.Power and Machines, Faculty of Eng, Ain-shams Univ. Cairo, Egypt.*

Hanyhasanien@ieee.org

Abstract— **Frequency fluctuation is a major concern for the transmission system operators (TSO) or power grid companies from the beginning of power system operation because it has some adverse effects on modern computer controlled industrial system, i.e., lamp flicker, inaccuracy of timing devices, etc. Because of huge penetration of wind power into the power grid, the frequency fluctuation is becoming a severe problem nowadays where randomly varying wind power causes the fluctuation of grid frequency of power system. Therefore, in this paper, the minimization of frequency fluctuation of power system including wind farm is proposed using energy capacitor system (ECS). A scaled down multi-machine power system model from Hokkaido prefecture, Japan, is considered for the analysis. A novel adaptive neural network (ANN) controller is considered for controlling the DC-bus connected ECS. The control objective is to smooth the line power of wind farm, taking into consideration the frequency deviation. The effects of wind power penetration levels as well as load variations are also analyzed. The proposed control method is verified by simulation analysis which is performed by PSCAD/EMTDC using real wind speed data. It is found that the adaptive neural network controlled ECS is an effective means to diminish the frequency fluctuation of multi-machine power system with connected wind farm.**

*Index Terms—***Energy capacitor system (ECS), electric double layer capacitor (EDLC), adaptive neural network (ANN), load frequency control (LFC), variable speed wind turbine (VSWT), permanent magnet synchronous generator (PMSG).**

I. INTRODUCTION

IN electrical power generation system, the present trend is to maximize the renewable energy penetration ratio as much as possible. Among the renewable energy sources such as wind, solar, biogas/biomass, tidal, geothermal, etc., wind energy has the huge potential to play an important role in energy market along with conventional energy sources. In 2008, 27 GW wind power has been installed all over the world, bringing world-wide installed capacity to 120.8 GW. This is 36% increase of the 2007 market, and represents about 28.8% increase of the global installed capacity [1]. However, the wind power fluctuates randomly because wind is intermittent and stochastic by nature. Therefore, huge penetration of the wind power into the grid raises the issue of power quality, which consequently deteriorates the quality of grid frequency.

The output power fluctuation of wind generators that causes the wide range frequency fluctuation has some adverse effects on the power system operation. For example, the frequency variation has bad effects on the computer controlled modern control systems widely used in industrial applications because it can cause erratic operation, data loss, system crashes, and equipment damage of computer. Lamp flickering is another outcome of the frequency fluctuation. It affects directly the human being. Moreover, the frequency fluctuation can cause the inaccuracy in the timing devices used in different home appliances as well as manufacturing equipments. It should be mentioned here that all the generating equipment in an electric system is designed to operate within very strict frequency margins. Grid codes specify that all the generating plants should be able to operate continuously between a frequency range around the nominal frequency of the grid, usually between 49.5 and 50.5 Hz in Europe [2, 3]. Some recent grid codes take into consideration the wind power integration issues stating that the wind farm must be disconnected without any time delay when it goes beyond the frequency band of 47.5–51.5 Hz [4]. Even within this band secondary frequency control or wind power reduction is necessary to maintain the frequency close to the nominal value [4]. Some other countries like Japan and South Korea impose more restriction on the wind farm operators to maintain the grid frequency. Therefore, necessary frequency restorative steps should be taken for the consideration of high penetration of wind power to the grid. In this study, a DC-bus coupled energy storage system (ESS) is proposed as the solution of mitigating short time frequency fluctuation in second range because of inclusion of randomly varying wind power to the power grid. In this study, energy capacitor system (ECS) is considered as the ESS. ECS consists of power electronic devices and electric

double layer capacitor (EDLC). An EDLC is a safer and has a longer life time than the secondary battery. Also, it requires almost no maintenance.

II. BACKGROUND OF THE STUDY

The integration of ESSs such as flywheel energy storage system (FESS), battery energy storage system (BESS), superconductive energy storage system (SMES) or energy capacitor system (ECS), to resolve the power fluctuation issue of wind farm is not a brand new concept [5-17]. In those studies, the energy storage unit is integrated to voltage source converter (VSC) or current source inverter (CSI) unit for the AC-DC conversion. However, VSC or CSI unit for AC-DC conversion increases the system cost and decreases the efficiency of the total system. In most of the studies [5-17], a simple power system model is considered where wind generator is connected to the infinite bus. For the analysis of wind farm power fluctuation, that model system including infinite bus is modest from the viewpoint of simplicity, though the frequency analysis necessitates more realistic model system without infinite bus. It is noted that the effects of governor control systems for the conventional generator units, such as load frequency control, governor free control and load limit operation, should be taken into consideration in frequency analysis for the sake of preciseness. Those attempts are not considered in the earlier studies. Again, except that most of the analysis is performed using the fixed speed wind generator. However, variable speed wind turbine generator system (WTGS) is becoming more popular than fixed speed one nowadays. In 2004, the world-wide market share of variable speed WTGS was more than 60% and it is growing more and more [18]. In our previous study [17], we reported a current controlled voltage source inverter (CCVSI) based ECS connected to the terminal of wind farm composed of variable speed wind generators. Though the control strategy was simple and suitable to integrate CCVSI with the variable speed wind generators, the cost issue for the power conversion unit could not be resolved. In this study, the aforementioned issues related to realistic model system, cost, and efficiency are taken into consideration, which even might be a benchmark model for future analysis.

In this study, frequency analysis is performed using a model system composed of fixed and variable speed wind turbine generator systems, hydro power generator, thermal power generators, nuclear power generator, and a load. This system is close to the real system. Load frequency control, governor free control,

and load limit operation are taken into consideration for the synchronous generator units. Each variable speed wind turbine (VSWT) driven permanent magnet synchronous generator (PMSG) unit in the wind farm is connected to the DC bus through individual generator side converter. The energy production cost for DC based wind farm is found lower than that for AC based wind farm as reported in [19]. The DC-bus is connected to the wind farm AC-bus through only one DC-AC inverter system. In this way, the number of DC-AC inverters and transformers necessary for connecting the wind farm to the grid can be decreased, and as a result the cost of overall system can also be reduced. The AC-DC converter of each VSWT-PMSG ensures the maximum power transfer to the DC-bus by using maximum power point tracking (MPPT) controller. The fixed speed wind generators are connected to the wind farm terminal. The necessary reactive power demand at the wind farm terminal is supplied from the DC-AC inverter system, and hence, the voltage can be maintained at the desired reference level set by transmission system operators (TSOs). Finally, the ECS is directly connected to the DC-bus using only a buck-boost DC-DC converter without any additional AC-DC conversion in order to reduce the system cost and increase the efficiency. The buck-boost DC-DC converter is widely used in industrial applications, which can provide smooth control, high efficiency and fast dynamic response. In this study, it is used to control the real power flow to and from the EDLC. A suitable control strategy based on adaptive neural network (ANN) is developed to smooth the wind farm line power as well as the grid frequency. The frequency deviation is also taken into consideration for designing ANN based ECS controller. This is one of the novel features of this work. The effect of different capacities of wind power penetration level on the frequency fluctuation is analyzed, along with load variations. Real wind speed data measured at Hokkaido Island, Japan, is considered in the simulation analysis. Extensive simulation results are presented. It can be noticed that the proposed control strategy can significantly diminish the effect of the wind power fluctuations on the system frequency.

III. MODEL SYSTEM

The model system used in the simulation analysis is shown in Fig. 1. It is a scaled down model of the power system of Hokkaido Island, Japan, which has the total capacity around 6.0 GW. The model system consists of a wind farm WF, a hydro power generator (HG) using a salient pole synchronous generator (SG1), two thermal power generators (TGs) using cylindrical type synchronous generators (SG2 and SG3),

a nuclear power generator (NG) using a cylindrical type synchronous generators (SG4), and a load. SG1 and SG2 are operated under load frequency control (LFC), SG3 is under Governor Free control (GFC) and SG4 is under Load Limit operation (LLO) [20]. In general, LFC is used to control frequency fluctuations with a long period more than a few minutes, and GFC is used to control fluctuations with a short period less than a minute. LLO is used to output constant power.

The wind farm consists of both fixed and variable speed WTGSs with the power capacity of 20 and 80 percentages of the total wind farm, respectively. Two variable speed wind turbine driven PMSGs are connected to the DC-bus through individual generator side converter. One DC-AC inverter system converts the DC voltage to AC grid voltage. Squirrel cage induction generator (IG) is considered as the fixed speed wind generator, which is connected to the wind farm terminal. A capacitor bank, C_{IGB}, is used for reactive power compensation of IG at steady state. The value of capacitor C_{IGB} is chosen so that power factor of the fixed speed wind generator during the rated operation becomes unity [21]. Another capacitor bank, C_{LoadB}, is considered to be connected at the load terminal to compensate the voltage drop by the impedance of transmission lines. Core saturations of induction generator and synchronous generators are not considered. Parameters of PMSGs, IG and SGs are shown in Table I. The base power of the main system is 100 MVA as shown in Fig.1. As different wind power penetration levels (5 and 10 MVA) are considered in the simulation analysis, the parameters of wind farm shown in Fig. 1 is expressed in per unit system using self capacity (WF capacity) base.

IV. AVR AND GOVERNOR MODELS FOR SYNCHRONOUS GENERATORS

A. Automatic voltage regulator (AVR)

AVR maintains the constant voltage at the terminal of synchronous generator, V_{t_SG}. In the simulation analysis, a simple AVR model is considered. It consists of a first order system as shown in Fig. 2a. The parameters of AVR are shown in Table II.

B. Governor for hydro, thermal and nuclear generators [20]

The governor unit automatically adjusts the rotational speed of the turbine and thus controls the generator output. When the generator load is constant, the turbine is operated at a constant rotational speed. However, when the load changes, balance between the generator output and the load is not maintained, and

therefore the rotational speed changes. When the load is removed, the governor detects the increase of the rotational speed, and the valve is closed immediately, so that an abnormal speed increase of the generator can be prevented.

The governor models used in the simulation analysis for hydro, thermal, and nuclear generators are shown in Fig. 2b and Fig. 2c [20]. The values of 65M and 77M are shown in Table III, where, Sg: the revolution speed deviation [pu]; 65M: the initial output [pu]; 77M: the load limit (65M + rated MW output × PLM[%]); PLM: the spare governor operation [%]; Pm: the turbine output [pu]. PLM for SG3 is set to 5[%]. For SG4 PLM is set -20[%] because the nuclear generator (SG4) output is controlled constant (load limit operation).

For Governor Free Control (GFC):

When PLM > 0

65M = the initial output [pu]

77M = 65M + rated MWoutput × PLM [%]

For Load Limit Operation (LLO):

When PLM < 0

65M = 77M+ rated MWoutput× | PLM[%] |

77M = the initial output [pu]

Sg is set to zero for SG1 and SG2 because these generators are operated under LFC to control frequency fluctuations with a relatively long period as explained below.

C. Load Frequency Control (LFC) Model [22], [23]

In the Load frequency control (LFC), the output power signal is sent to each power plant when the frequency deviation is detected in the power system. Then, governor output value (65M) of each power plant is changed by LFC signals, and the power plant output is changed. A second order low pass filter (LPF) removes the short period fluctuations of the frequency deviation signal, because the LFC is used to control frequency fluctuations with a long period. The LFC model is shown in Fig. 2d, where, T_c is the LFC period = 200[s]; ω_c is the LFC frequency = $1/T_c$ = 0.005[Hz] and ζ is the damping ratio = 1.

V. Wind Turbine Modeling

The mathematical relation for the mechanical power extraction from the wind can be expressed as follows [24]:

$$P_w = 0.5\rho\pi R^2 V_w^{\;3} C_P(\lambda,\beta) \tag{1}$$

where P_w is the extracted power from the wind, ρ is the air density [kg/m^3], R is the blade radius [m], V_w is the wind speed [m/s] and C_p is the power coefficient which is a function of both tip speed ratio, λ, and blade pitch angle, β [deg]. Both fixed speed (FSWT) and variable speed wind turbine (VSWT) characteristics used in this study are chosen from [24-26]. The maximum power point tracking (MPPT) strategy explained in [21] is adopted in this study.

VI. Control Strategy of the Wind Farm

Each of converter/inverter used with variable speed WTGS is a standard 3-phase two-level unit, composed of six IGBTs and anti-parallel diodes. For the generator side converter, the well known cascaded control is considered. As the converter is directly connected to the PMSG, its q-axis current is proportional to the active power. The active power reference of the converter is determined in such a way to provide the maximum power to the grid through the common DC-bus. The d-axis stator current is proportional to the reactive power. The reactive power reference is set to zero to perform unity power factor operation. Also, for the operation of grid side inverter the cascaded control is considered. The dc-link voltage can be controlled by the d-axis current. The rated dc-link voltage is 2.3 kV, in this study. On the other hand, the reactive power of grid-side inverter can be controlled by the q-axis current. The reactive power reference is set in such a way that the terminal voltage of the wind farm remains constant. Therefore, the voltage stability of wind farm can be ensured by the reactive power compensation from grid-side inverter. Moreover, as the fixed speed wind generators are connected to the terminal of grid-side inverter, the voltage fluctuation due to the fixed speed wind generator can also be mitigated by the grid side inverter. The details of the generator side converter and grid side inverter are available in [17].

VII. Modeling and Control Strategy of ECS

In this study, energy capacitor system (ECS) composed of DC-DC buck/boost converter and EDLC bank

is considered to be connected to the common DC-bus of the model system as shown in Fig. 1. The schematic diagram of ECS is shown in Fig. 3a. The buck/boost converter controls the real power of ECS.

A. Modeling of EDLC

The distributed model of EDLC bank shown in Fig. 3b is considered in the simulation analysis. It can represent the terminal characteristics of the EDLC cell precisely [15]. The rated EDLC bank voltage is chosen 2.3 kV. The rated capacity of the EDLC bank is 5.0 MW, 0.097 MWh. The parameters of the EDLC bank are shown in Table IV.

B. Control Strategy of DC-DC Buck/Boost Converter

A DC-DC converter which has a bi-directional power flow capability is required in the control of EDLC. In this work, the DC-DC buck/boost converter shown in the dashed line in Fig. 3c is considered. It operates alternately by controlling switches g_1 and g_2 to be ON or OFF. Care must be taken to ensure that the two switches are not fired together; otherwise, the DC bus voltage will be short-circuited.

As the objective of using ECS is to minimize the frequency fluctuations caused by randomly varying wind generator output, the control strategy is to smooth the wind farm line power. At the beginning an initial reference power, P_{ref}, is obtained from the simple moving average (SMA) of wind farm total output obtained from both fixed and variable speed wind generators. All the generators in the wind farm are not running at the same speed. Therefore it is logical to generate reference power from the wind farm total output power, which will be used in the control of DC-DC buck/boost converter. In this work, 180 sec (60 periods each of 3 sec) SMA is used to generate the P_{ref} [21]. The adaptive neural network (ANN) controller controls the duty cycle based on the reference signal. To obtain good and fast smoothing performance, the frequency deviation signal is incorporated with P_{ref} to some extent. A multiplying constant, G, is considered to accelerate the convergence speed. Finally, the revised reference signal, P_{ref_rev} and wind farm line power are chosen as the control inputs of the ANN. If the line power is greater than the modified reference power, the EDLC will be charged, and the DC-DC converter will work on buck converter mode. Also, if the line power is lower than the modified reference power, the EDLC will be discharged, and the DC-DC converter will work on boost converter mode. Gate signals are determined using the duty cycle control as shown in Fig. 3c. The duty cycle is compared with the sawtooth carrier wave to generate the gate signals for buck-

boost DC-DC converter. The frequency of the sawtooth carrier signal is chosen to be 250 Hz. The details of the proposed adaptive neural network (ANN) controller are described in the following section.

VIII. The adaptive artificial neural network controller

Classical control theory suffers from some limitations due to the assumptions made in designing the control systems such as linearity, time-invariance, etc. Essentially, the conventional proportional-integral (PI) and proportional-integral-derivative (PID) controllers have been utilized in many control applications due to the robustness of these controllers and they offer a wide stability margin. However, the conventional PI and PID controllers are very sensitive to parameter variations and nonlinearity of dynamic systems. Setting of the parameters of the PI controllers used in cascaded control is cumbersome, especially in power system application which is difficult to express by a mathematical model or transfer function. These problems can be overcome by using artificial intelligence based control techniques. Such control systems can also be less sensitive to parameter variation than classical control systems [27].

In recent years, fuzzy logic control and artificial neural networks techniques have been applied to the control of nonlinear dynamic systems. Unlike classical control strategies, fuzzy logic incorporates an alternative way of thinking, but based on the experience of the designer in tuning the membership functions [28]. Neural controllers implemented on a microprocessor have a simple code and very short processing time compared with fuzzy controllers. Control surfaces obtained from neural controllers also do not exhibit the roughness of fuzzy controllers that can lead to unstable or raw control. One severe disadvantage of a fuzzy system is its limited ability of handling problems with multiple inputs [29]. The main drawback of neural controllers is that the design process is more complicated than that of fuzzy controllers. However, this difficulty can be easily overcome with proper design tools. The main advantages of the ANN controllers are as follow:

❑   Their design does not require the mathematical model of the plant.

❑   They can lead to improve performance, when properly tuned.

❑   They may require less tuning effort than conventional controllers [27].

Though the ANN controllers can handle the characteristics of nonlinearity but it may suffer from the convergence time and the long training process. Therefore, in this study, the adaptive ANN controller is

presented. The proposed controller ensures fast and accurate dynamic response with an excellent steady state performance.

A. Description of ANN

ANN controllers are models of computation based on an analogy with biological neural networks. Biological neural networks can learn from experience and it follows that many ANN models can learn, also. Usually, an ANN consists of a highly parallel ensemble of simple computing elements, or neurons. Further, neurons usually have many interconnections with other neurons in the ANN. One class of ANN interconnection strategies is the feedforward strategy. The class of feedforward ANN structure is used in our study. Relevant ANN model design considerations are the selection of inputs, the number of hidden layers, the number of neurons in each hidden layer and tuning the weights of ANN.

The input vector of the ANN controller consists of the revised reference line power, P_{ref_rev}, line power of wind farm, $P_L(t)$, and the output signal of the ANN controller u(t). The inputs of the ANN controller have to be carefully chosen, as this dictates the boundness and stability of the desired trajectories. The selection of number of hidden layers, and the number of neurons in each hidden layer is performed by trial and error, which is the most commonly used method in ANN architecture design. A three layer feedforward neural structure with three neurons in one hidden layer is found to be a good balance between estimation error and ANN complexity. The ANN structure with $3 \times 3 \times 1$ (three neurons in input layer, three neurons in hidden layer, and one neuron in output layer) is shown in Fig. 4. The input nodes are selected as equal to the number of input signals and the output node equals to the number of output signal.

The output of a single neuron can be represented by the following equation:

$$a_i = f_i\left(\sum_{j=1}^{n} w_{ij} x_j(t) + b_i \right) \tag{2}$$

where, f_i is the activation function, w_{ij} is the weighting factor, x_j is the input signal, and b_i is the bias. The most commonly used activation functions are non-linear, continuously varying types between two asymptotic values -1 and +1. They are called tansigmoid function. The activation function used is the tansigmoid function in both hidden and output layers.

B. Learning Algorithm

The adaptive ANN controller is based on the Widrow-Hoff adaptation algorithm. The Widrow-Hoff

delta rule can be used to adapt the adaline's weight vector [30]. The weight update equation for the original form of the algorithm can be written as:

$$W(t+1) = W(t) + \alpha \frac{e_p(t).x(t)}{|x(t)|^2} \tag{3}$$

where, $W(t+1)$ is the next value of the weight vector, $W(t)$ is the present value of the weight vector, and $x(t)$ is the present input vector. The present power error $e_p(t)$ is defined to be the difference between the line power signal $P_L(t)$ and the revised reference line power P_{ref_rev}.

Changing the weights yields a corresponding change in the error:

$$\Delta e_p(t) = \Delta(P_{ref\_rev} - P_L(t)) = -x^T(t)\Delta W(t) \tag{4}$$

In accordance with the Widrow-Hoff delta rule of eq. (3), the weight change is as follows:

$$\Delta W(t) = W(t+1) - W(t) = \alpha \frac{e_p(t).x(t)}{|x(t)|^2} \tag{5}$$

Combining Equations (4) and (5), we obtain

$$\Delta e_p(t) = -\alpha \frac{e_p(t).x^T(t).x(t)}{|x(t)|^2} = -\alpha.e_p(t) \tag{6}$$

Therefore, the error is reduced by a factor of α as the weights are changed while holding the input pattern fixed. Presenting a new input pattern starts the next adaptation cycle. The next error is then reduced by a factor of α, and the process continues. The initial weight vector is usually chosen to be zero and is adapted until convergence. The choice of α controls stability and speed of convergence. The power error converges if and only if $0 < \alpha < 2$. Making α greater than 1 generally does not make sense, since the error would be overcorrected. The total error correction comes with $\alpha = 1$. The practical range for α is usually between 0.1 and 1.

This Widrow-Hoff adaptation algorithm is self-normalizing in the sense that the choice of α does not depend on the magnitude of the signals. The weight update is collinear with the input pattern and of a magnitude inversely proportional to $|x(t)|^2$. The desired error correction is achieved with a weight change of the smallest possible magnitude.

The Widrow-Hoff adaptation algorithm is used to adapt both all the weighting factors between the input and hidden layers and all the weighting factors between the hidden and output layers. Therefore, the ANN controller in our study is fully adaptive controller [31].

The output signal of the adaptive ANN controller u(t) after being rescaled is used to generate the duty cycle according to the following equation.

$$D_{new} = D_{old} + k.u \tag{7}$$

where, D_{old} is the one step time delayed duty cycle signal and k is a multiplying constant.

Thus, The proposed algorithm corrects error and it minimizes the mean square error between the desired revised reference line power P_{ref_rev} and the actual line power $P_L(t)$ over all times. The algorithm is best known for this property.

IX. SIMULATION ANALYSIS

Real wind speed data is measured from a 275 kW wind turbine located at Hokkaido Island, Japan, as shown in Fig. 5a. Data with wide wind speed variation is shorted out and used in both fixed and variable speed wind turbines. This is to ensure obtaining large frequency fluctuation which is needed to validate the effectiveness of the proposed control scheme to minimize grid frequency fluctuation caused by wind farm. The step time and simulation time are chosen to be 0.00002 s and 500 s, respectively. Simulations results are carried out by using PSCAD/EMTDC [32]. In the simulation study, four different cases are considered with different wind power penetration levels and load conditions as shown in Table V. Case 1 and case 2 are for heavy and light load conditions, respectively, when the wind power penetration level is moderate. Cases 3 and 4 are for heavy and light load conditions, respectively, when the wind power penetration level is high. The governor control strategy for hydro, thermal, and nuclear generators during heavy and light load conditions are shown in Table III. During the light load condition the hydro generator is considered out of generation.

The wind farm output power for the aforementioned cases are shown in Fig. 5b. Cases 1 and 2 and cases 3 and 4 overlaps as power levels are kept constant as given in Table V. Because of the random fluctuation of wind power, the grid frequency fluctuates as shown in Figs. 5c and 5d. Though in Fig. 5b, wind power fluctuation was in the same level for heavy and light load conditions both for moderate and high wind power penetration conditions, the frequency fluctuations are not the same as can be seen from Figs. 5c and 5d. It can be noticed that with the same wind power penetration level (for cases 1 and 2 or cases 3 and 4), the light load condition faces more severe frequency fluctuation than that of the heavy load condition.

Moreover, the frequency fluctuations become severe as the wind power penetration level increases. It is noted that as thermal power generator, hydro generator, and nuclear power generator hold the major share compared to the wind generators, the impact on frequency is more for those conventional generators. However, focus is given on frequency fluctuation caused by wind power plant, in this study. Since the frequency fluctuates most severely for the case-4 compared to other 3 cases, it is chosen as the base case for the study of frequency fluctuation minimization using ANN controlled ECS.

The response of wind farm line power for case-4 is shown in Fig. 6a with and without considering ANN controlled ECS. It can be realized that the wind farm line power can be smoothed considerably when ANN controlled ECS is adopted. The proposed controller can precisely control the real power to and from the ECS as required by the system. If the line power is greater than the modified reference power as mentioned in Sect. VII.B, the ECS can absorb real power and store it into EDLC bank. Again, if the line power is lower than the modified reference power, the ECS can provide real power and discharge electric energy from EDLC bank. The real power response of ECS is shown in Fig. 6b. As a result of the wind farm line power smoothing, it can be noticed that the grid frequency fluctuations is minimized as shown in Fig. 6c. Therefore, the ANN controlled ECS ensures suppression of frequency fluctuations of wind farm connected power system. The responses of synchronous generators in service for Case-4 considering ANN controlled ECS are shown in Fig. 6d. In general, the output of SG3 fluctuates widely because this generator is operated under GFC in order to control the electric power fluctuations with short period. However, under the proposed control strategy that oscillation is also reduced as shown in Fig. 6d. It is noted that the grid side inverter of PMSG wind generators can control the reactive power properly. As a result, the terminal voltage can be maintained constant at the desired level set by Transmission System Operators (TSOs) for the cases with and without ECS as shown in Fig. 7a. The responses of common DC-bus voltage and EDLC bank voltage are shown together in Fig. 7b. The DC bus voltage is maintained constant by the frequency converter of the variable speed wind turbine driven permanent magnet synchronous generator, but the EDLC bank voltage varies during charging/discharging by the proposed ANN controller.

In the simulation analysis, conventional pitch controllers are considered for both cases with and without considering ECS. However, an advanced pitch control strategy can be considered to smooth the wind generator output power as well as frequency fluctuation as reported in [33] up to a certain extent where the

wind turbine mechanical power above the reference power is not extracted by controlling the blade pitch angle of wind turbines. However, this type of control reduced the captured power and might be applicable during low load condition only. In light of the simulation analysis, it can be realized that the ANN controlled ECS can effectively handle the frequency fluctuation issue of wind farm connected power system.

X. CONCLUSION

The wind power penetration level to the power grid is increasing day by day almost linearly. Due to this the power system security and reliability are being threatened from the view point of frequency fluctuation, which is the ultimate outcome of random wind power variation. The frequency fluctuation is directly affecting the human being by lamp flickering as well as creating miscellaneous problem in computer controlled industrial system and timing devices. This study first demonstrated the range of frequency variation due to random wind variation using a realistic model system under different load and wind power penetration conditions. Then an adaptive neural network controlled ECS is a newly applied to mitigate the frequency fluctuation of the grid system. The proposed controller has ensured fast and accurate dynamic response for the grid connected wind farm. It is found that the ANN controlled ECS is an effective means to minimize the frequency fluctuation caused by the wind farm output. This also ensures the compatibility of wind farm to the recent grid codes. Consequently, it can improve the power quality and reliability of the power system.

XI. ACKNOWLEDGMENT

XII. REFERENCES

[1] The Global Wind Energy Council, GWEC Latest News, 2009, "US and China in race to the top of global wind industry," February, 2009, [Online], http://www.gwec.net/

[2] Standard EN 50160- Voltage Characteristics in Public Distribution Systems, July 2004, [Online], http://www.leonardo-energy.org/webfm_send/2703

[3] Inigo Martinez de Alegria, Jon Andreu, Jose Luis Martin, Pedro Ibanez, Jose Luis Villate, Haritza Camblong, "Connection requirements for wind farms: A survey on technical requirements and regulation," Renewable and Sustainable Energy Reviews, Vol.11, Issue 8, pp. 1858–1872, 2007.

[4] B.Singh and S.N.Singh, "Wind Power Interconnection into the Power System: A Review of Grid Code Requirements," The Electricity Journal, Vol.22, Issue 5, pp. 54–63, 2009.

[5] F. Hardan, J.A.M Bleijs, R. Jones, P. Bromley, and A.J. Ruddell, "Application of a power-controlled flywheel drive for wind power conditioning in a wind/diesel power system," Ninth International Conference on Electrical Machines and Drives, paper No. 468, pp.65-70, Canterbury, 1999.

[6] R. Cardenas, R. Pena, G. Asher, and J. Clare, "Power smoothing in wind generation systems using a sensorless vector controlled induction Machine driving a flywheel," IEEE Trans. on Energy Conversion, Vol.19, Issue.1, pp. 206 - 216, 2004.

[7] R. Takahashi, Wu. Li; T. Murata, and J. Tamura, "An Application of Flywheel Energy Storage System for Wind Energy Conversion," International Conference on Power Electronics and Drives Systems, (PEDS 2005), pp. 932-937, Nov. 2005.

[8] S. M. Muyeen, Mohd. Hasan Ali, R. Takahashi, T.Murata, and J.Tamura, "Wind Generator Output Power Smoothing and Terminal Voltage Regulation by Using STATCOM/ESS," CD Record of the IEEE PowerTech 2007 conference, Paper No. 258, Lausanne, Switzerland, July 2007.

[9] M. EL Mokadem, C. Nichita, P. Reghem, and B. Dakyo, "Wind Diesel System for DC Bus Coupling With Battery and Flywheel storage," XVII International Conference on Electrical Machines (ICEM-06), Paper ID. 699, Chania, Greece, 2006.

[10] M.H.Ali, T.Murata, J.Tamura, "Minimization of Fluctuations of Line Power and Terminal Voltage of Wind Generator by Fuzzy Logic-Controlled SMES," International Review of Electrical Engineering (I.R.E.E.), Vol.1, No.4, pp.559-566, 2006/10.

[11] T. Kinjo, T. Senjyu, N. Urasaki, and H. Fujita, " Terminal-voltage and output-power regulation of wind-turbine generator by series and parallel compensation using SMES," IEE Proc.-Gener. Transm. Distrib., Vol.153, No.3, pp.276-282, May 2006.

[12] T. Asao, R. Takahashi, T. Murata, and J. Tamura, "Smoothing Control of Wind Power Generator Output by Superconducting Magnetic Energy Storage System," Proceeding of International Conference on Electrical Machines and Systems 2007 (ICEMS07), pp.303-307, Seoul, Korea, 2007.

[13] M.. H. Ali, J. Tamura, and B. Wu, "SMES strategy to minimize frequency fluctuations of wind generator system," 34th Annual Conference of IEEE Industrial Electronics,(IECON2008), pp. 3382-3387, 2008.

[14] Li Wei Li, G. Joos, C. Abbey, "Wind Power Impact on System Frequency Deviation and an ESS based Power Filtering Algorithm Solution," IEEE PES Power Systems Conference and Exposition (PSCE), pp.2077 – 2084, 2006.

[15] T. Kinjo, T. Senjyu, N. Urasaki, and H. Fujita, "Output levelling of renewable energy by electric double-layer capacitor applied for energy storage system," IEEE Trans. on Energy Conversion, Vol. 21, Issue.1, pp. 221-227, 2006.

[16] S. M. Muyeen, S. Shishido, Mohd. Hasan Ali, R. Takahashi, T. Murata, and J.Tamura, "Application of Energy Capacitor System (ECS) to Wind Power Generation," Wind Energy, Vol. 11, No. 4, pp. 335-350, DOI: 10.1002/we.265, July/August 2008.

[17] S. M. Muyeen, R. Takahashi, T. Murata, and J.Tamura, "Integration of Energy Capacitor System with Variable Speed Wind Generator," IEEE Trans. on Energy Conversion, Vol.24, No.3, pp.740-749, 2009.

[18] F. V. hulle, "Large Scale Integration of Wind Energy in the European Power Supply Analysis, Issue and Recommendations," EWEA, Tech. Rep., December 2005.

[19] Stefan Lundberg, "Evaluation of wind farm layouts," Nordic Workshop on Power and Industrial Electronics (NORPIE), Poster No. 2693, Norway, June 2004.

[20] Inst. Electrical Engineers of Japan (IEEJ), Technical Reports, "Standard Models of Electrical Power System," Vol.754, pp.1-82, 1999.

[21] S. M. Muyeen, J. Tamura, and T. Murata, "Stability Augmentation of a Grid-connected Wind Farm," Springer-Verlag London, ISBN 978-1-84800-315-6, October 2008.

[22] T.Inoue, "MW Response of Thermal Power Plant from Viewpoint of Power System Frequency Control," IEEJ Trans. on Power and Energy, Vol.124-B, No3, pp. 343-346, 2004.

[23] A.Murakami, A.Yokuyama, Y.Tada, "Basic Study on Battery Capacity Evaluation for Frequency Control in Power System with a Large Penetration of Wind Power Generation," IEEJ Trans. on Power and Energy, Vol.126-B, No. 2, pp. 236-242, 2006.

[24] S. Heier, Grid Integration of Wind Energy Conversion System, Chicester, UK, John Wiley & Sons Ltd., 1998.

[25] O. Wasynczuk, D. T. Man, J. P. Sullivan, "Dynamic behavior of a class of wind turbine generator during random wind fluctuations," IEEE Trans. on Power Apparatus and Systems, Vol. PAS-100, No.6, pp.2873-2845, 1981.

[26] J. G. Slootweg, S. W. H. De Hann, H. Polinder, W. L. Kling, "General Model for Representing Variable Speed Wind Turbines in Power System Dynamic Simulations," IEEE Trans. on Power System, Vol.18, No.1, 2003.

[27] Muhammad H Rashid, "Power Electronics Handbook", reference book, Second edition, Elsevier Inc, 2007.

[28] Ahmed Rubaai, Daniel Ricketts, and M. David Kankam, "Development and implementation of an adaptive Fuzzy-Neural-Network controller for brushless drives", *IEEE Transactions on Industry Applications*, vol. 38, No. 2, pp. 441-447. March/April 2002.

[29] J. Binfet and B.M. Wilamowski, "Microprocessor implementation of fuzzy systems and neural networks," Proceedings of International Joint Conference on Neural Networks (IJCNN'01), Vol.1, pp.234-239, USA, 2001.

[30] B. Widrow and M. A. Lehr, "30 years of adaptive neural networks: Perceptron, madaline, and backpropagation," in *Proc. IEEE,* vol. 78, pp. 1415-1442, Sept. 1990.

[31] Hany M. Hasanien, "FPGA implementation of adaptive ANN controller for speed regulation of permanent magnet stepper motor drives," Energy Conversion and Management, vol. 52, issue 2, pp. 1252-1257, Feb. 2011.

[32] PSCAD/EMTDC Manual, Manitoba HVDC Research Center, April 2005.

[33] S. M. Muyeen, Mohd. Hasan Ali, R. Takahashi, T. Murata, and J.Tamura, "Wind Generator Output Power Smoothing by Using Pitch Controller," International Review of Electrical Engineering (I.R.E.E.), Vol.2, No.3, pp.310-321, 2007.
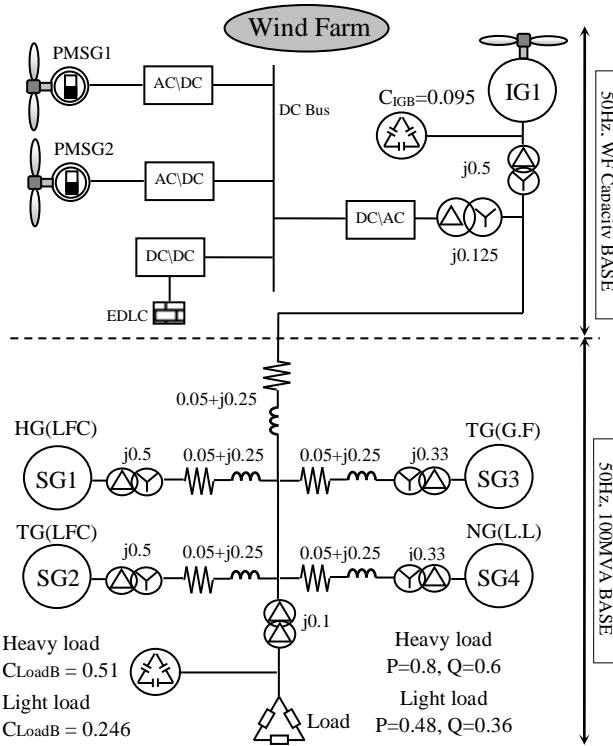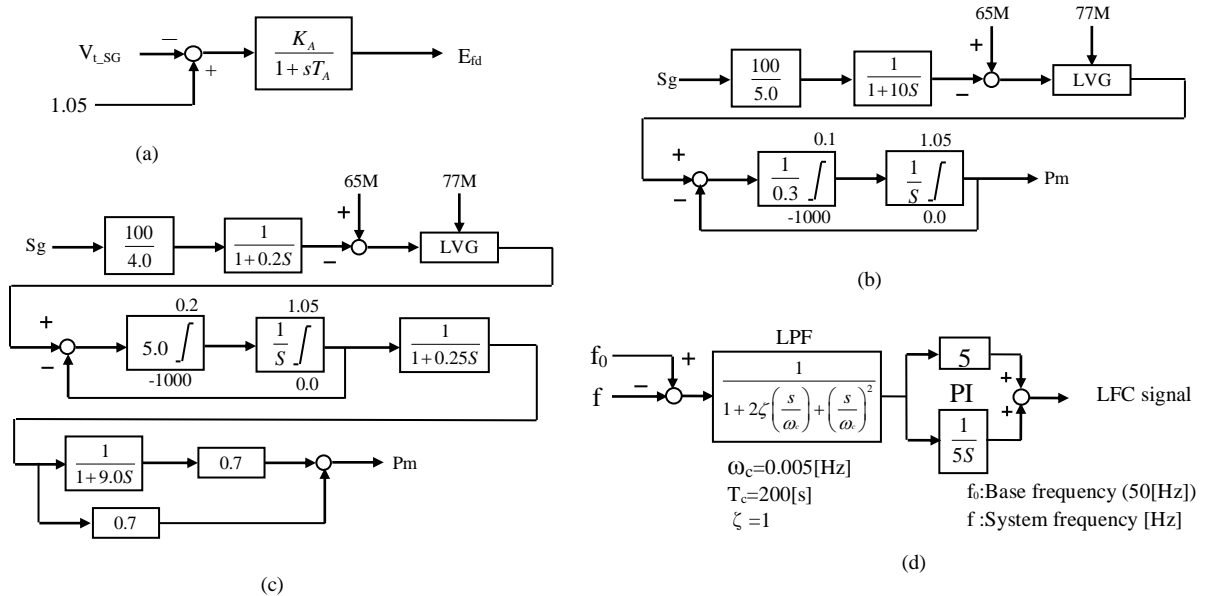
Fig.1 Model System

(a)

(b)

(c)

(d)

Fig. 2. Block diagram used in synchronous generators (a) AVR, (b) hydro governor, (c) thermal and nuclear governor, (d) LFC model
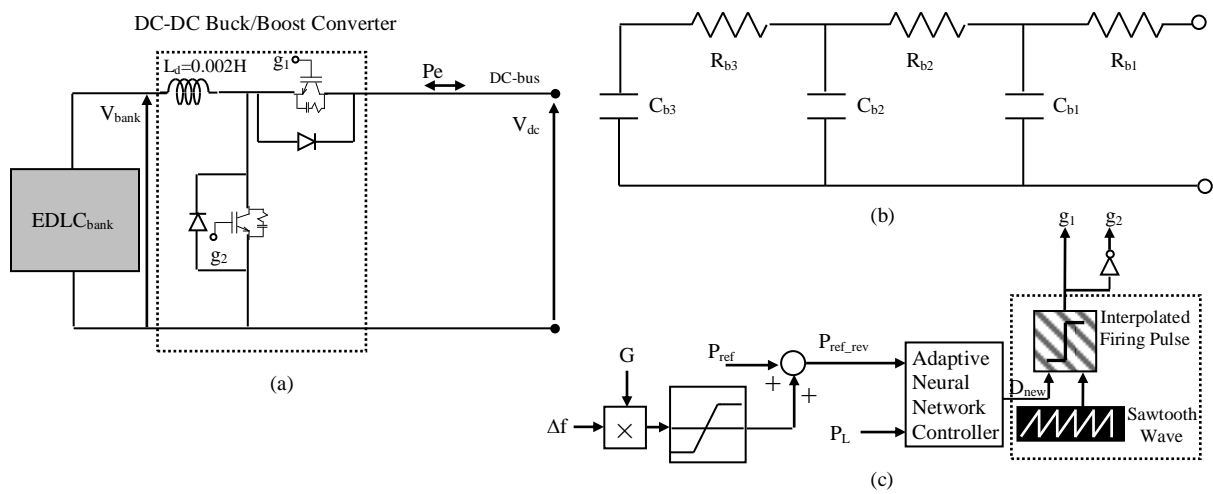
Fig. 3. ECS modeling and control (a) schematic diagram, (b) distributed model of EDLC bank, (c) control block of DC-DC buck/boost converter
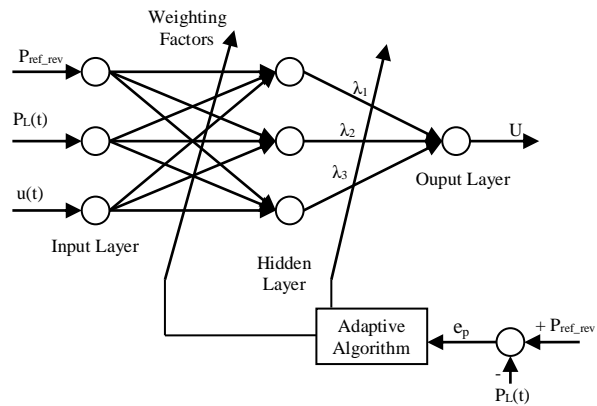

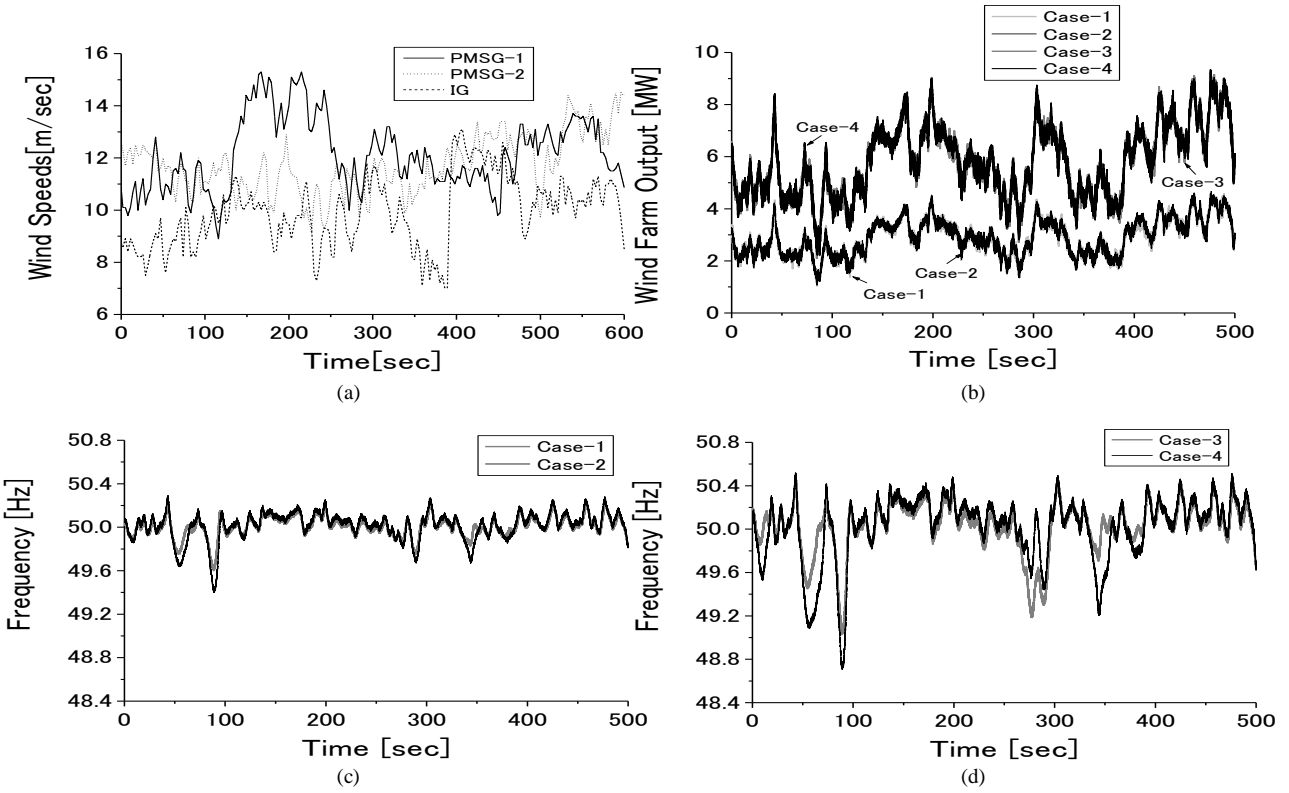Fig. 4. Adaptive artificial neural network structure

(a)

(b)

(c)

(d)

Fig. 5. Responses without ECS (a) wind speeds, (b) wind farm output power, (c) grid frequency for cases 1 &2, (d) grid frequency for cases 3&4
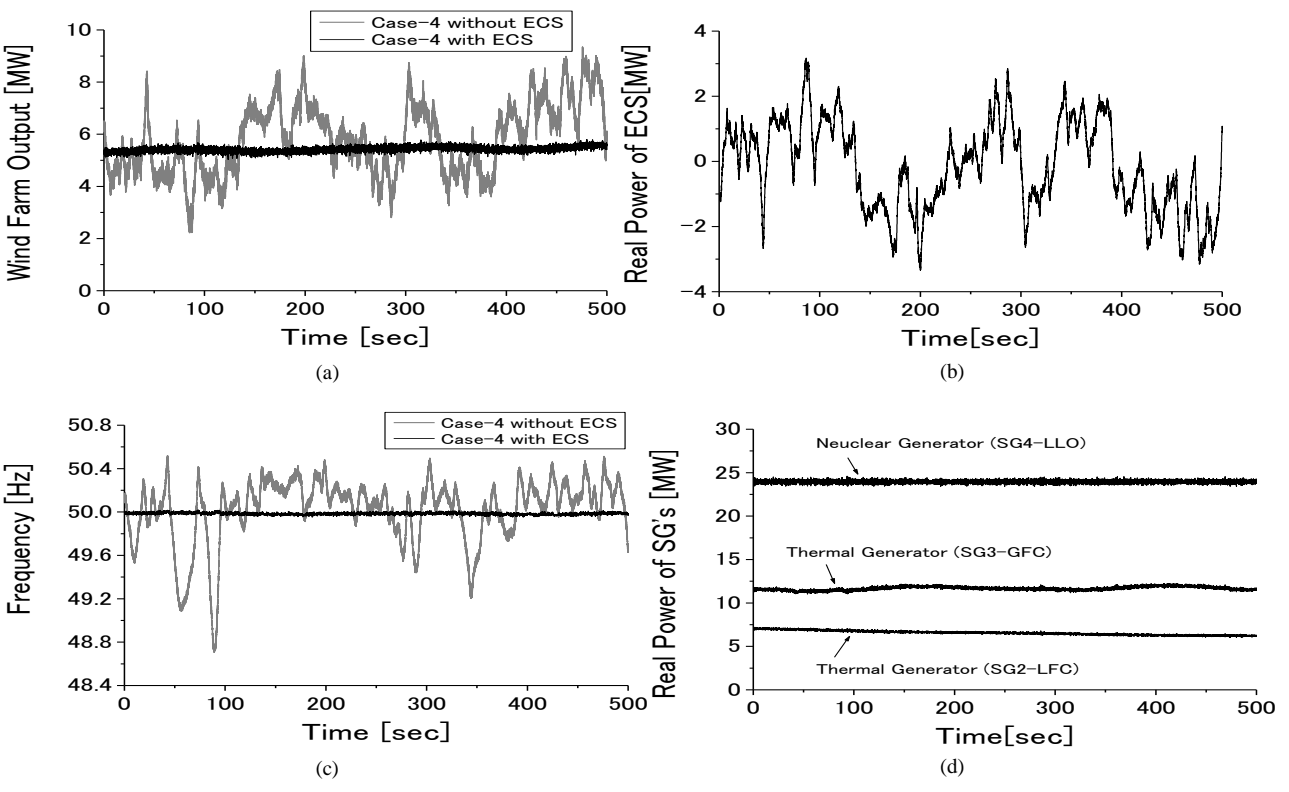

(a)

(b)

(c)

(d)

Fig. 6. Smoothing effect by using ECS (a) wind farm output power, (b) real power of ECS, (c) grid frequency, (d) real power of SGs
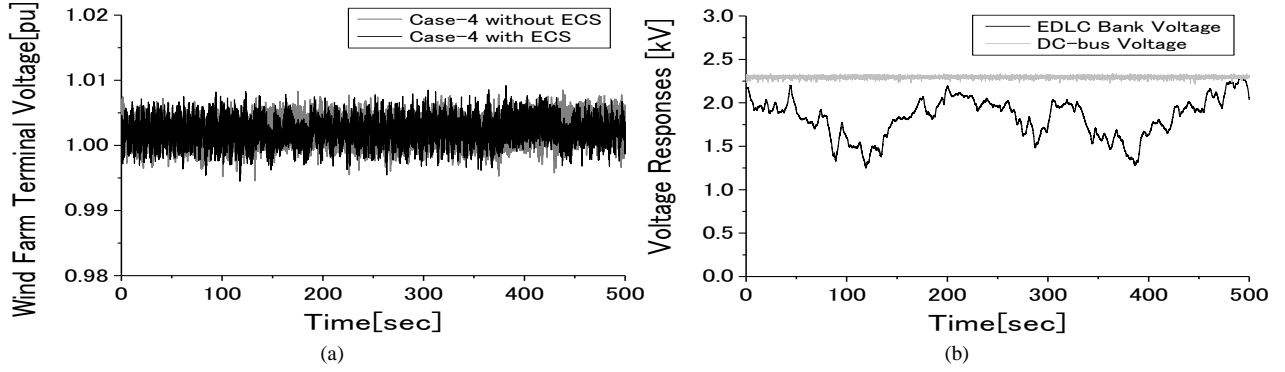

(a)

(b)

Fig. 7. Other responses (a) wind farm terminal voltage, (b) DC voltage responses

TABLE I
PARAMETERS OF GENERATOR

Permanent Magnet Synchronous Generator (PMSG)			
MVA		2 or 4	
V [kV]	1.0	Xd [pu]	1.0
f [Hz]	20	Xq [pu]	0.7
p	150	Φ [pu]	1.4
R1 [pu]	0.01	H [s]	3.0
Induction Generator (IG)			
MVA	1 or 2		
r_1 [pu]	0.01		
x_1 [pu]	0.1		
x_{mu} [pu]	3.5		
r_{21} [pu]	0.035		
x_{21} [pu]	0.03		
r_{22} [pu]	0.014		
x_{22} [pu]	0.098		
H [s]	1.5		
Synchronous Generator			
	Salient pole type	Cylindrical rotor type	
	SG1	SG2	SG3	SG4
MVA	20	20	30	30
Xd [pu]	1.2	2.11		
Xq [pu]	0.7	2.02		
2H [s]	2.5	2.32		

TABLE II
PARAMETERS OF AVR

Gain K_A	400
Time Constant T_A [s]	0.02

TABLE III
VALUES OF 65M AND 77M

SG1(Hydro)			SG2(Thermal)		
Frequency control	65M	77M	Frequency control	65M	77M
LFC(Load=100MVA)	LFC Signal	1	LFC(Load=100MVA)	LFC signal	1
LFC(Load=60MVA)	✕		LFC(Load=60MVA)		
SG3(Thermal)			SG4(Nuclear)		
Frequency control	65M	77M	Frequency control	65M	77M
GF(Load=100MVA)	0.8	0.84	LL(Load=100MVA)	0.96	0.8
GF(Load=60MVA)	0.4	0.42	LL(Load=60MVA)		

TABLE IV
DETAILED MODEL PARAMETERS OF EDLC BANK

Capacitance		Internal Resistance	
C_{b1}	2.9F	R_{b1}	0.00748Ω
C_{b2}	72.58F	R_{b2}	0.187Ω
C_{b3}	69.68F	R_{b3}	0.179Ω

TABLE V
CASE STUDY

Cases	Wind farm output power penetration level (MVA)	Load condition (MVA)
Case-1	5(PMSG1=2;PMSG2=2;IG=1)	100
Case-2	5(PMSG1=2;PMSG2=2;IG=1)	60
Case-3	10(PMSG1=4;PMSG2=4;IG=2)	100
Case-4	10(PMSG1=4;PMSG2=4;IG=2)	60